Universiteit
Leiden
The Netherlands

Molecular and Nano-engineering with iron, ruthenium and carbon: Hybrid structures for sensing

Geest, E.P. van

Cover Page

Universiteit Leiden

The handle http://hdl.handle.net/1887/139187 holds various files of this Leiden University dissertation.

Author: Geest, E.P. van
Title: Molecular and Nano-engineering with iron, ruthenium and carbon: Hybrid structures for sensing
Issue Date: 2021-01-14

Chapter 6

Reducing the translocation speed of DNA in solid-state nanopores by photolabile ruthenium complex decoration

Nanopores in thin membranes are useful for detecting single DNA molecules. So far, the major drawback of solid-state nanopores is that the translocation speed of DNA is too high to sequence the DNA strand. We decorated DNA with ruthenium complexes that stay bound in the dark but are released upon visible light irradiation. As demonstrated with single nucleotides, the ruthenium complex $[Ru(tpy)(biq)(OH_2)]^{2+}$, obtained by the hydrolysis of $[Ru(tpy)(biq)Cl]Cl$, coordinates specifically to guanosine nucleotides in the dark, and the formed complex releases the nucleotide upon green light irradiation. When Ru-functionalized DNA translocated through a nanopore in silicon nitride, the translocation speed of this decorated strand was not significantly changed compared to non-functionalized DNA, but the ionic current blockade was higher. Our results showed that the ruthenium complexes co-translocated with DNA, which led to stronger DNA detection signals. We envision that if the ruthenium complex would be fixed to the surface of the pore-containing membrane, the photolabile binding of DNA to the metal may be used to control the translocation speed of DNA using light.

6.1. Introduction

In 2015 a major breakthrough in DNA sequencing was made when Oxford Nanopore Technologies introduced MiniON, the first commercially available DNA-sequencing device.[1] The MiniON, which uses biological nanopores (membrane proteins embedded in lipid membranes) for DNA sequencing, demonstrated that nanopores can be used as sequencing devices for human genome sequencing.[2] Next to biological nanopores, solid-state nanopores are an appealing alternative for DNA sequencing devices as they can be precisely shaped and fabricated on a large scale, have high mechanical robustness, and good chemical and thermal resilience.[3]

In spite of its potential, DNA sequencing in solid-state nanopores has not been accomplished so far. A major challenge for solid-state nanopore sequencing is to reduce the velocity at which each DNA translocates through the pore. For double-stranded DNA, a translocation speed of ~30 bases/µs was measured, meaning a single base resides in the pore for only 20 nanoseconds, a time too short for precise identification of each base pair.[4] The translocation speed could already be lowered by one order of magnitude through tuning the viscosity of the solutions, which increases friction.[5] Yet, also in this case DNA could still move at relatively high speed though the pore, thus preventing precise DNA sequencing using this type of devices.

Herein, we propose an alternative method to slow down the translocation of DNA as it passes through a solid-state nanopore. Ruthenium complexes are known to be able to bind to DNA via the formation of coordination bonds.[6, 7] Importantly, the ruthenium-purine coordination bond can be photolabile if the right ruthenium polypyridyl complex is chosen,[8] so that the coordination equilibrium between DNA and ruthenium in the dark may thus be shifted by irradiation with visible light. We hypothesized that when the DNA is decorated with the bulky ruthenium complexes, the translocation speed of the strand would decrease as the complexes may provide additional friction in the nanopore. As the number of complexes that are attached to the DNA strand can be varied by simply varying the light intensity, simultaneously the friction of the DNA strand and thus the translocation speed can be controlled with light (see Figure 6.1).
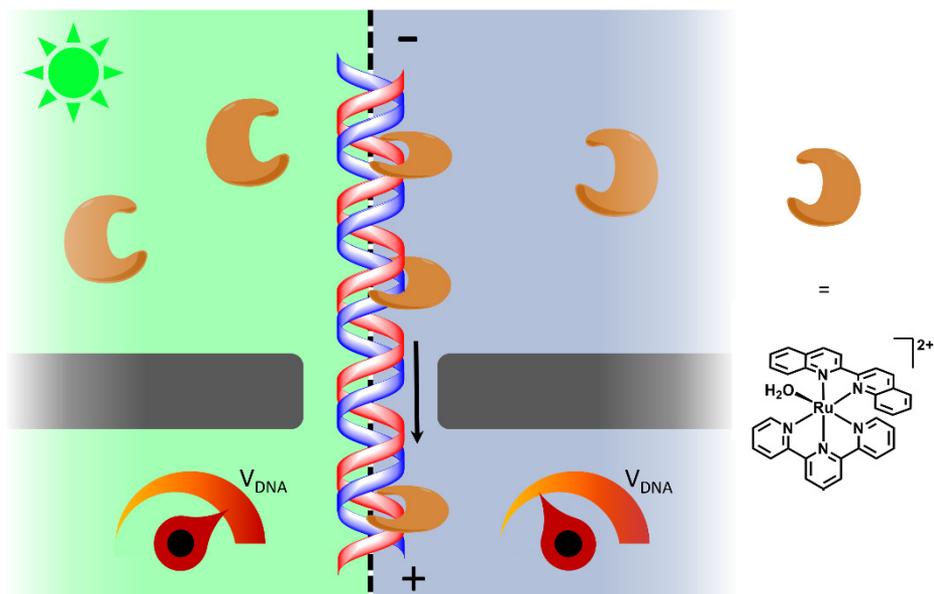
Figure 6.1: **Ruthenium-decorated DNA in a nanopore device**. A nanopore separates two chambers of the flow cell filled with electrolyte. When a potential is applied over the membrane, DNA translocates through the nanopore. The anchored ruthenium complex coordinates to DNA in the dark (right, grey) and slows down the translocation speed of the DNA strand, while the ruthenium complexes can be removed from the DNA again through visible light irradiation (green, left).

6.2. Results and Discussion

6.2.1. Light-sensitive ruthenium-nucleotide interactions

The ruthenium complex [Ru(tpy)(biq)Cl]Cl ([**1**]Cl), where tpy = 2,2':6'2''-terpyridine and biq = 2,2'-biquinoline, was synthesized using reported methods,[9] and the interactions of this complex with the four nucleotides (see Scheme 6.1A), *i.e.* 2-deoxyadenosine monophosphate (dAMP), 2-deoxythymidine monophosphate (dTMP), 2-deoxycytidine monophosphate (dCMP) and 2-deoxyguanosine monophosphate (dGMP), and with DNA were studied with UV-vis spectroscopy to investigate the interaction of the ruthenium complex with DNA. When complex [**1**]Cl is dissolved in demineralized water, the coordinated Cl ligand dissociates, yielding the aqua complex [Ru(tpy)(biq)(OH$_2$)]$^{2+}$ ([**2**]$^{2+}$),[10] which can engage with different coordination reactions, for example with nucleotides (see Scheme 6.1B).

A

dAMP dTMP dCMP dGMP

B
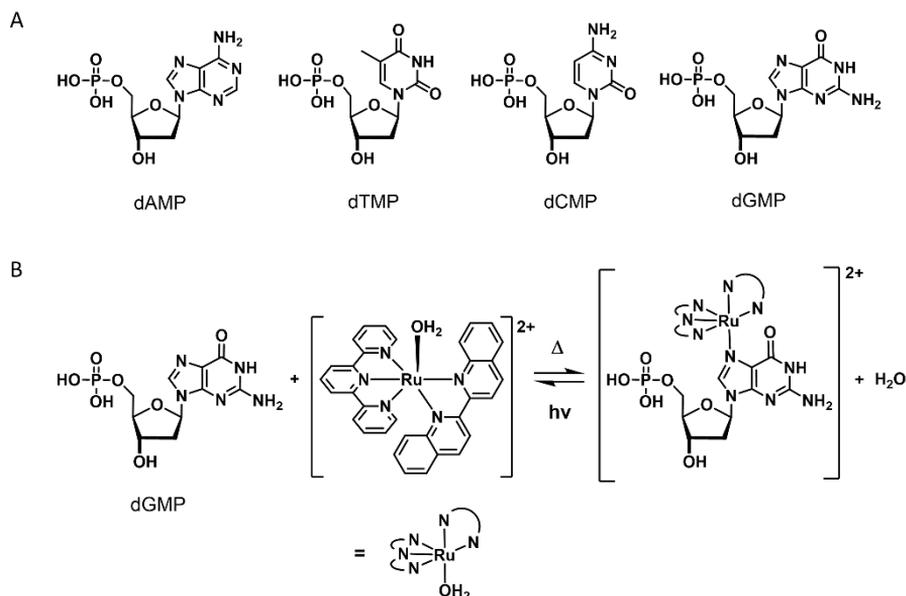
dGMP

Scheme 6.1: Reaction of complex [2]²⁺ with nucleotides. A) Structure of the four model DNA nucleotides used in this work. B) Interconversion between the aqua complex [2]²⁺ and its dGMP analogue [3]²⁺. This equilibrium is shifted towards the formation of [3]²⁺ in the dark, but towards the formation of [2]²⁺ under visible light irradiation.

Mass spectroscopy showed that the reaction of dGMP with [2]²⁺ results in the formation of [Ru(tpy)(biq)(dGMP)]²⁺ ([3]²⁺) by the appearance of a peak at m/z = 937.0, *i.e.* [3 - H]⁺. The coordination of dGMP could simply be reversed by irradiation of the reaction mixture with visible light (530 nm): the peak at m/z = 937.0 was no longer present after irradiation. UV-vis spectroscopy showed a shift from 546 to 549 nm of the metal-to-ligand charge transfer (MLCT) band from the ruthenium complex and a clear isosbestic point at 540 nm, indicating a direct conversion of the dGMP species [3]²⁺ to the aqua complex [2]²⁺ (see Figure 6.2A and Figure S6.1). Furthermore, UV-vis showed that this reaction is selective for dGMP; compound [2]²⁺ does not react with the other nucleotides dAMP, dTMP and dCMP in the same conditions, which is in agreement with the selectivity for dGMP reported for a similar ruthenium complex, [Ru(tpy)(bpy)Cl]PF₆ (bpy = 2,2′-bipyridine).[11]

When complex [2]²⁺ was mixed with calf thymus DNA (ctDNA) in water, the coordination of double-stranded DNA to the ruthenium center was again observed with UV-vis spectroscopy, as well as the photodriven release of DNA. This behavior was similar to the (photo)reactivity of [2]²⁺ in presence of dGMP

(see Figure 6.2B). The nucleotides in a DNA strand can thus still interact with the ruthenium complex. As the coordination reaction of [**2**]$^{2+}$ with nucleotides was selective for dGMP, we assume that in ctDNA the guanine nucleobases selectively coordinate to the ruthenium complex, likely through binding of the N7 position, which is typically the preferred binding site for ruthenium complexes.[7, 12] Importantly, the binding is reversed by light irradiation, giving control over the loading of the DNA fragment with ruthenium complexes.
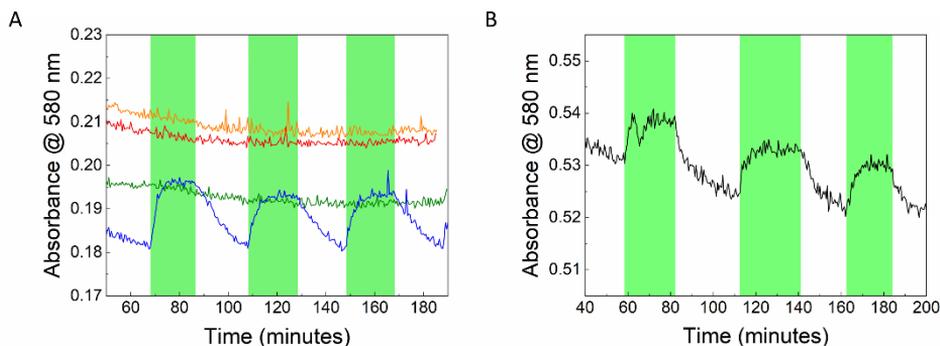
Figure 6.2: UV-vis study of the interactions between [2]$^{2+}$ and nucleotides or DNA. A) Evolution of the absorbance of solutions of [**2**]$^{2+}$ + dAMP, dTMP, dCMP or dGMP (red, orange, green and blue, respectively, [Ru] = 50 μM, [nucleotide] = 250 μM) in water, either in the dark or upon irradiation with light (530 nm, *P* = 5.64 mW). Temperature: 37 °C. Irradiation periods are indicated by green regions. B) Evolution of the absorbance of a solution of [**2**]$^{2+}$ + calf thymus DNA (black, [Ru] = 50 μM, [ctDNA] = 100 μM) in water, either in the dark or upon irradiation with light (530 nm, *P* = 5.64 mW). Temperature: 37 °C. Irradiation periods are indicated by the green regions.

6.2.2. Ruthenium-decorated DNA in nanopore devices

After we confirmed that [**2**]$^{2+}$ is able to bind to DNA and release again upon irradiation, we used the ruthenium complex for nanopore translocation measurements. First, nanopores had to be fabricated; solid-state nanopores in silicon nitride chips (SiN, membrane thickness = 30 nm) were fabricated in situ. The nanopore setup, in which the chip was mounted, consisted of a *cis* and *trans* chamber both filled with an ionic solution (KCl), and separated by the SiN membrane of the chip (see Chapter 1, Figure 1.3). A hole in the membrane was produced by dielectric breakdown, which by applying a large potential over the membrane creates a pore at the weakest point in the thin silicon nitride membrane through electrical etching, ultimately connecting the two chambers.[13] Once the electrical etching was complete, as seen from a strong drop of the electrical resistance *R* between the *cis* and *trans* chamber, the current was cut to prevent

further etching. The approximate diameter of the pore could be determined by measuring R between the *cis* and *trans* chamber after the pore was created (larger pores give smaller values for R),[14] and was typically in the order of tens of nanometer.

DNA detection measurements were done using the nanopore setup with ruthenium-decorated DNA. To ensure coordination of ruthenium, λ-DNA (linear, 48502 base pairs, from *E. coli* bacteriophage λ; 10 ng/μL) was first incubated with [**2**]²⁺ in the dark to allow the ruthenium to bind to the DNA strand. As a reference, λ-DNA (10 ng/μL) was used that was not incubated with the metal complex. The DNA solutions were injected in the *cis* chamber, where the strands with their negative phosphate backbones were driven through the pore by applying a positive potential from the *trans* chamber. While DNA translocated, the ionic current over the SiN membrane was measured, which was then correlated to the pore diameter; smaller pores gave lower ionic currents. Translocation of individual molecules in the pore, in this case DNA (either with or without ruthenium), causes a narrowing of the pore that leads to a current blockade (see Figure 6.3A), and represents so-called translocation events.[15]

Typically, ionic current data were acquired for several minutes in order to detect several hundreds of events (bare λ-DNA: 295 events; Ru-incubated λ-DNA: 321 events). For each event the magnitude of the current blockade and the duration of translocation, also called "dwell time", was recorded. Interestingly, the histogram of event frequency *vs.* current blockade showed that the binding of the ruthenium complex to DNA had a strong effect on the translocation events. Although the dwell time statistical distribution was identical in presence and in absence of the ruthenium complex, always in the range of a few milliseconds (1.29 +/- 0.67 and 1.48 +/- 0.81 milliseconds, respectively, see Figure 6.3B), current blockades were typically higher when the ruthenium complex was coordinated to the DNA strands (see Figure 6.3C). While bare λ-DNA led to a statistical distribution of current blockade characterized by a single maximum at 256 ± 46 pA, Ru-incubated λ-DNA, on the other hand, led to a distribution with not one but two maxima at higher current blockades (320 ± 38 pA and 573 ± 83 pA, see Figure 6.3D). Thus, the presence of the ruthenium complex did not significantly affect the dwell time, however it did increase the magnitude of the ionic current blockade.
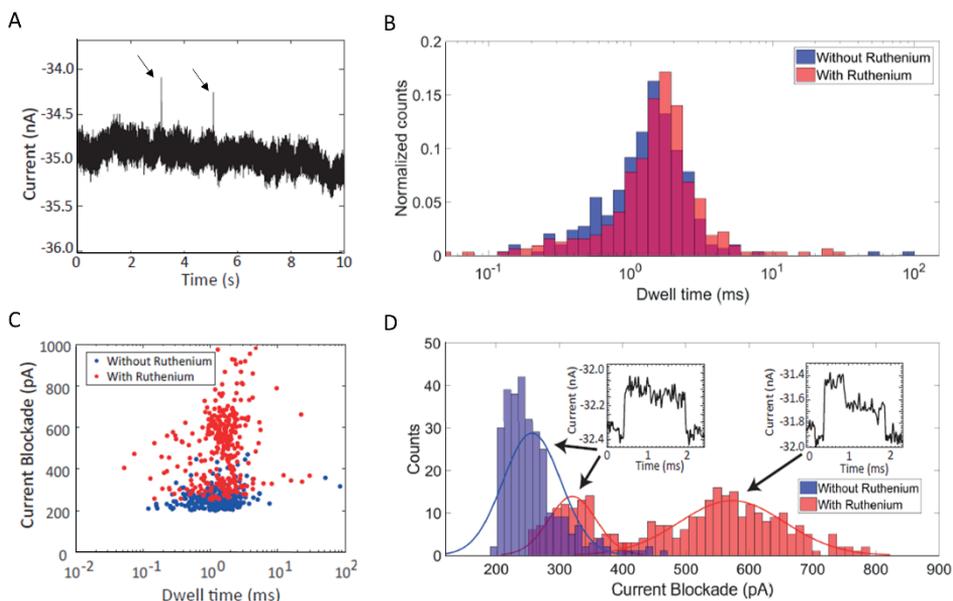
Figure 6.3: Event detection with a 40 nm nanopore in silicon nitride. A) Typical ionic current trace measured with a ± 40 nm sized nanopore after addition of DNA. Two translocation events are visible as upward peaks (indicated by arrows). Applied voltage: -100 mV, pH = 8. All experiments were done in 1 M KCl buffered with 10 mM Tris and 1 mM EDTA. B) Dwell time histogram of the translocation events for bare DNA (blue) and DNA incubated with [2]$^{2+}$ (red). C) Scatterplot of all detected events of bare λ-DNA (N = 295, blue) and λ-DNA incubated with complex [2]$^{2+}$ (N = 321, red). D) Current blockade histogram of the events with corresponding normal distribution fits for bare DNA (blue) and DNA incubated with [2]$^{2+}$ (red). The insets show two types of translocation events. The arrows show in which part of the current blockade distribution these event types were found.

The existence of the two peaks in the current blockade histogram (Figure 6.3D) obtained in presence of [2]$^{2+}$ indicates that there were two types of DNA molecules that passed through the nanopores. One interpretation is that the DNA did not maintain a single average shape in the presence of complex [2]$^{2+}$, but that there were two conformations that gave rise to two different ion current profiles upon translocation; indeed, ruthenium complexes are known to be able to induce conformational changes in DNA.[16] More information about the possible different conformations of DNA in presence of complex [2]$^{2+}$ could be obtained from the detailed ion current *vs.* time profile of each translocation event. For λ-DNA without [2]$^{2+}$ and for the low-current blockade events (between 250 and 400 pA) obtained with Ru-incubated λ-DNA, a continuous current plateau was observed until the strand had travelled through the pore, while for high-current blockade events obtained with Ru-incubated λ-DNA (between 400 and 800 pA), an increase to a first plateau was accompanied by a drop to a second plateau in the ion

current, before the strand left the pore and the current dropped back to the baseline (see Figure 6.3D, insets). This current drop could be due to folding of the DNA strand; a folded strand would provide a larger blockade of the pore and thus a higher ion current blockade (see Figure 6.4A); complex [2]$^{2+}$ appears to promote folding of the DNA strand. Why this folding occurs only in presence of [2]$^{2+}$ and only for the larger current blockades is not obvious. The folding could be due to electrostatic interactions of Ru^{2+} with the negatively charged phosphate backbone of DNA. Bridging of Ru between DNA by coordination only is very unlikely, as only one site is available for the coordination of a DNA base pair to the complex. Possibly, the coordinated ruthenium gives the DNA strand a positive charge, to which the negative backbone of the same strand binds by electrostatic forces (Figure 6.4B).
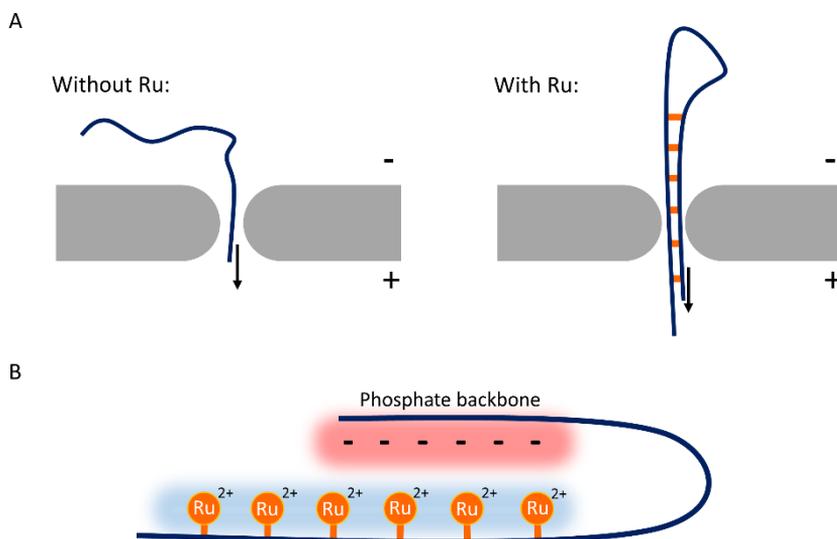
Figure 6.4: Schematic representation of folded DNA in a nanopore. A) While the undecorated DNA strand appears to be linear when it translocates through the pore (left), the larger ionic current for ruthenium-decorated DNA indicated that DNA could be folded (right). B) When a DNA strand is decorated with ruthenium complexes, the positive charges of the complexes could be involved in electrostatic interaction with the phosphate backbone, causing the DNA to fold.

Overall, the presence of the ruthenium complex [2]$^{2+}$ did not affect the dwell time of translocation events, but increased the current blockade in DNA detection experiments, likely because the conformation of the DNA changed, possibly by folding. Based on these experiments and the UV-vis results, we believe that the ruthenium complex co-translocated with the DNA through the nanopore.

6.3. Conclusions & Outlook

Ruthenium complex [**2**]²⁺, which is obtained by hydrolysis of [**1**]Cl in aqueous solutions, binds to DNA specifically on the dGMP nucleotides according to UV-vis spectroscopy. This coordination interaction was found to be an equilibrium, which upon green light irradiation (530 nm) can be shifted towards the aqua complex [**2**]²⁺. Thermal binding and photodriven dissociation of dGMP or guanine nucleobases in DNA could be cycled several times with limited decomposition. During translocation of λ-DNA through a nanopore in a silicon nitride membrane (30 nm thickness), the current blockade with a DNA strand pre-incubated with [**2**]²⁺ was higher than with bare λ-DNA, while the dwell time remained unaffected. We hypothesized that ruthenium co-translocated with the DNA strand, making the DNA more bulky, which increased the current blockade as a larger portion of the pore was blocked by the DNA strands. However, the time spent in the pore by each translocating DNA fragment did not change upon ruthenium binding. These results present a first step towards nanopores that are covalently functionalized with ruthenium complexes like [**2**]²⁺ that are able to bind to DNA in the dark and slow down translocation, and unbind upon visible light irradiation. Ultimately, shining visible light onto such systems may be used to control the translocation speed of DNA by shifting the binding equilibrium of [**2**]²⁺ to the DNA fragment.

6.4. Acknowledgements

6.5. References and Notes

[1]   M. Jain, H. E. Olsen, B. Paten, M. Akeson, *Genome Biol.* **2016**, *17*, 239.
[2]   R. Bowden, R. W. Davies, A. Heger, A. T. Pagnamenta, M. de Cesare, L. E. Oikkonen, D. Parkes, C. Freeman, F. Dhalla, S. Y. Patel, N. Popitsch, C. L. C. Ip, H. E. Roberts, S. Salatino, H. Lockstone, G. Lunter, J. C. Taylor, D. Buck, M. A. Simpson, P. Donnelly, *Nat. Commun.* **2019**, *10*, 1869; M. Jain, S. Koren, K. H. Miga, J. Quick, A. C. Rand, T. A. Sasani, J. R. Tyson, A. D. Beggs, A. T. Dilthey,

I. T. Fiddes, S. Malla, H. Marriott, T. Nieto, J. O'Grady, H. E. Olsen, B. S. Pedersen, A. Rhie, H. Richardson, A. R. Quinlan, T. P. Snutch, L. Tee, B. Paten, A. M. Phillippy, J. T. Simpson, N. J. Loman, M. Loose, *Nat. Biotechnol.* **2018**, *36*, 338.

[3]   F. Haque, J. Li, H.-C. Wu, X.-J. Liang, P. Guo, *Nano Today* **2013**, *8*, 56; Y. Goto, R. Akahori, I. Yanagi, K.-i. Takeda, *J. Hum. Genet.* **2020**, *65*, 69; M. Wanunu, *Phys. Life Rev.* **2012**, *9*, 125.

[4]   B. Luan, G. Stolovitzky, G. Martyna, *Nanoscale* **2012**, *4*, 1068.

[5]   D. Fologea, J. Uplinger, B. Thomas, D. S. McNabb, J. Li, *Nano Lett.* **2005**, *5*, 1734.

[6]   H.-K. Liu, S. J. Berners-Price, F. Wang, J. A. Parkinson, J. Xu, J. Bella, P. J. Sadler, *Angew. Chem., Int. Ed.* **2006**, *45*, 8153; P. M. van Vliet, S. M. Toekimin, J. G. Haasnoot, J. Reedijk, O. Nováková, O. Vrána, V. Brabec, *Inorg. Chim. Acta* **1995**, *231*, 57; N. Grover, T. W. Welch, T. A. Fairley, M. Cory, H. H. Thorp, *Inorg. Chem.* **1994**, *33*, 3544; O. Novakova, H. Chen, O. Vrana, A. Rodger, P. J. Sadler, V. Brabec, *Biochemistry* **2003**, *42*, 11544.

[7]   S. Liu, A. Liang, K. Wu, W. Zeng, Q. Luo, F. Wang, *Int. J. Mol. Sci.* **2018**, *19*.

[8]   H. Chan, J. B. Ghrayche, J. Wei, A. K. Renfrew, *Eur. J. Inorg. Chem.* **2017**, *2017*, 1679.

[9]   L. N. Lameijer, D. Ernst, S. L. Hopkins, M. S. Meijer, S. H. C. Askes, S. E. Le Dévédec, S. Bonnet, *Angew. Chem., Int. Ed.* **2017**, *56*, 11549.

[10]   A. Bahreman, B. Limburg, M. A. Siegler, E. Bouwman, S. Bonnet, *Inorg. Chem.* **2013**, *52*, 9456.

[11]   J. Rodríguez, J. Mosquera, J. R. Couceiro, M. E. Vázquez, J. L. Mascareñas, *Angew. Chem., Int. Ed.* **2016**, *55*, 15615.

[12]   Z. Adhireksan, G. E. Davey, P. Campomanes, M. Groessl, C. M. Clavel, H. Yu, A. A. Nazarov, C. H. F. Yeo, W. H. Ang, P. Dröge, U. Rothlisberger, P. J. Dyson, C. A. Davey, *Nat. Commun.* **2014**, *5*, 3462; R. E. Morris, R. E. Aird, P. D. Murdoch, H. M. Chen, J. Cummings, N. D. Hughes, S. Parsons, A. Parkin, G. Boyd, D. I. Jodrell, P. J. Sadler, *J. Med. Chem.* **2001**, *44*, 3616; H. Chen, J. A. Parkinson, R. E. Morris, P. J. Sadler, *J. Am. Chem. Soc.* **2003**, *125*, 173.

[13]   H. Kwok, K. Briggs, V. Tabard-Cossa, *PLOS ONE* **2014**, *9*, e92880; K. Briggs, M. Charron, H. Kwok, T. Le, S. Chahal, J. Bustamante, M. Waugh, V. Tabard-Cossa, *Nanotechnology* **2015**, *26*, 084004.

[14]   A. Fragasso, S. Pud, C. Dekker, *Nanotechnology* **2019**, *30*, 395202; S. W. Kowalczyk, A. Y. Grosberg, Y. Rabin, C. Dekker, *Nanotechnology* **2011**, *22*, 315101.

[15]   C. Plesa, C. Dekker, *Nanotechnology* **2015**, *26*, 084003.

[16]   O. Novakova, J. Kasparkova, V. Bursova, C. Hofr, M. Vojtiskova, H. Chen, P. J. Sadler, V. Brabec, *Chem. Biol.* **2005**, *12*, 121.